

Creating highly symmetric qudit heralded entanglement through highly symmetric graphs

Seungbeom Chin ^{*1}

¹Department of Electrical and Computer Engineering, Sungkyunkwan University, Suwon 16419, Korea

April 9, 2024

Abstract

Recent attention has turned to exploring quantum information within larger Hilbert spaces by utilizing qudits, which offer increased information capacity and potential for robust quantum communications. While the efficient generation of multipartite qudit entanglement is crucial for studying quantum correlations in high-dimensional Hilbert spaces, the increased dimension makes the circuit design challenging, especially when the entanglement is generated by heralding detections. In this work, we demonstrate that the graph picture of linear quantum networks (LQG picture) can provide a simplified method to generate qudit multipartite heralded entanglement of high symmetries. The LQG picture enables the reduction of circuit complexity by directly imposing the state symmetry onto the circuit structure. Leveraging this insight, we propose heralded schemes for generating N -partite N -level anti-symmetric (singlet) and symmetric (Dicke) states. Our study shed light on the optimal circuit design of high-dimensional entanglement with a systematic graphical strategy.

1 Introduction

The quantum information science has significantly impacted contemporary technological advancement. Extensive research has been conducted in this field, yielding remarkable outcomes in quantum computing [1–3], communication [4, 5], and simulation [6]. The fundamental unit of quantum information is a qubit, which is constructed with a two-level quantum system and serves as the quantum equivalent of the classical bit. It presents intriguing potential to explore quantum information within larger Hilbert spaces, which include a larger number of qubits or higher-level quantum systems that correspond to *qudits*. Quantum information processing based on qudits recently draw attention by its increased capacity compared to qubits and potential to execute more robust and secure quantum communications [7, 8]. For the study of high-dimensional Hilbert space, it is essential to find efficient schemes for generating multipartite qudit entanglement with realistic quantum particles.

One promising method for tackling this task involves leveraging the indistinguishability of quantum particles. Several studies have proposed both theoretical and experimental schemes for generating entanglement, utilizing the identity of quantum particles with postselection (see, e.g., [9–14]). However, in postselected schemes, the generation of the target state is confirmed only after the detection of particles, which makes the resource less suitable for consecutive quantum gate operations. This limitation serves as significant motivation for investigating heralded schemes [15–22], which integrate ancillary particles and modes to indicate the successful generation of target states. This approach enables the selection of experimental runs that yield the desired target states without directly measuring them. Consequently, the entanglement produced through heralded schemes becomes more handy resource that is not destructed by detectors. Heralded entangled states are also considered useful for loophole-free Bell violation tests by their robust structures against lossy channels [23, 24].

Nevertheless, heralded schemes typically require much more particles and modes for heralding resources, rendering them more intricate to design compared to postselected schemes. To overcome this

*sbthesy@skku.edu

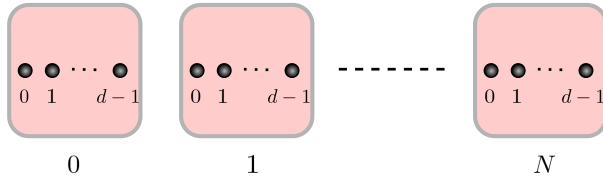


Figure 1: The initial boson distribution of dN bosons in the qudit sculpting protocol. Each spatial mode from 1 to N has d bosons, whose internal states are mutually orthogonal with each other, i.e. $|0\rangle, |1\rangle, \dots, |d-1\rangle$.

limitation of heralded schemes, a graph-based approach for generating heralded entanglement is introduced Ref. [20–22], which establish a framework wherein many-particle systems, including boson annihilation operators, are mapped to bipartite graphs (bigraphs). This is an extension of the graph picture introduced in Ref. [25]. Since there are other several graphical methods to understand quantum information processing [26–29], we term our method the *linear quantum graph (LQG) picture* to avoid confusion.

In this work, we exploit the LQG picture to find intriguing and valuable qudit multipartite entangled states with heralding. The circuit complexity increases substantially when we increase the dimension of Hilbert space and simultaneously choose heralding instead of postselection. However, when the state has a highly symmetric structure, the LQG picture provides a powerful insight to reduce the design complexity by directly imposing the state symmetry to the circuit itself. One of such examples is the qudit GHZ state generating scheme proposed in Ref. [20], which shares the same cyclic symmetry with the target state. We suggest heralded schemes for generating N -partite N -level symmetric and anti-symmetric states based on the property.

The N -partite N -level anti-symmetric (singlet) state $|\mathcal{S}_N\rangle$ is written as

$$|\mathcal{S}_N\rangle \equiv \frac{1}{\sqrt{N!}} \sum_{\sigma \in S_N} \text{sgn}(\sigma) |\sigma(0), \sigma(1), \dots, \sigma(N-1)\rangle \quad (1)$$

(S_N is the permutation group and $\text{sgn}(\sigma)$ is the signature of σ), which is known to be useful resource for, e.g., the problems of N -strangers, secret sharing, liar detection [30], and byzantine agreement [31].

Among several types of qudit Dicke states (see, e.g., Ref. [32] for the definition), we focus on the following state:

$$|D^N(\underbrace{1, 1, \dots, 1}_N)\rangle \equiv \frac{1}{\sqrt{N!}} \sum_{\sigma \in S_N} |\sigma(0), \sigma(1), \dots, \sigma(N-1)\rangle, \quad (2)$$

which is one of the states that has the largest minimal decomposition entropy [33] and useful for quantum communication and metrology [34].

So far as we know, there have been no scheme for the heralded generations of the N -partite N -level totally symmetric and anti-symmetric states. For the case of $|\mathcal{S}_N\rangle$, there are a few attempts to generate the state with quantum nondemolition (QND) measurements [35, 36], however they are restricted by the low efficiency of QND detectors. On the other hand, our scheme consist of linear transformation operators and conventional number-resolution detector, hence more feasible.

2 LQG picture of d -level Qudit entanglement generation with boson subtractions

We design our heralded schemes following the *d -level boson sculpting protocol*, which is presented in Ref. [20] by generalizing the the 2-level boson sculpting protocol [37].

In our system, bosons are in j th spatial mode ($j \in \{1, 2, \dots, N\}$) with a d -dimensional internal degree of freedom s ($\in \{0, \dots, d-1\}$), hence we denote the boson creation (annihilation) operators as $\hat{a}_{j,s}^\dagger$ ($\hat{a}_{j,s}$). To create N -partite d -level entanglement, we first allocate dN bosons into N spatial modes

Boson systems with a sculpting operator	Bipartite graph $G_b = (U \cup V, E)$
Spatial modes	Labelled vertices $\in U$
$\hat{A}^{(l)}$ ($l \in \{1, 2, \dots, N\}$)	Unlabelled vertices $\in V$
Spatial distributions of $\hat{A}^{(l)}$	Edges $\in E$
Probability amplitude $\alpha_j^{(l)}$	Edge weight $\alpha_j^{(l)}$
Internal state $\psi_j^{(l)}$	Edge weight $\psi_j^{(l)}$

Table 1: Correspondence relations of a sculpting operator to a sculpting bigraph

evenly as in Fig. 1, which is represented in the operational form by

$$|Sym_{N,d}\rangle \equiv \prod_{j=1}^N (\hat{a}_{j,0} \hat{a}_{j,1} \cdots \hat{a}_{j,d}) |vac\rangle. \quad (3)$$

Then we subtract $(d-1)N$ bosons from the N -partite system with a sculpting operator $\hat{A}_N = \prod_{l=1}^{(d-1)N} \hat{A}^{(l)}$ so that it subtracts $(d-1)$ particles per mode. Hence the final state is given by

$$|\Psi\rangle_{fin} = \hat{A}_N |Sym_{N,d}\rangle \quad (4)$$

Then each particle remaining in each mode constitutes qudit information. A suitable sculpting operator generates a genuine multipartite entangled state.

The LQG picture of the sculpting operator is suggested in Ref. [20], which is displayed in Table 1. For a clear visibility of graphs, we employ a simplified notation for edge weights. More specifically, in this work we consider only cases when all the absolute values of probability amplitude weights are equal among those which are attached to the same dot. Hence, we omit the probability amplitude weights when the phase of the probability amplitude is 0, and denote phase (not amplitude) otherwise. In addition, we work in a computational basis $\{0, 1, \dots, d-1\}$ and its Fourier-transformed basis $\{\tilde{0}, \tilde{1}, \dots, \tilde{d-1}\}$ in our approach, which can be replaced with edge colors. We set $\tilde{0}$ = Red and $\tilde{d-1}$ = Blue in this work.

Now we provide a crucial property of bigraphs that is essential to design qudit multipartite entanglement: For a bigraph, if edges are attached to all the circles as



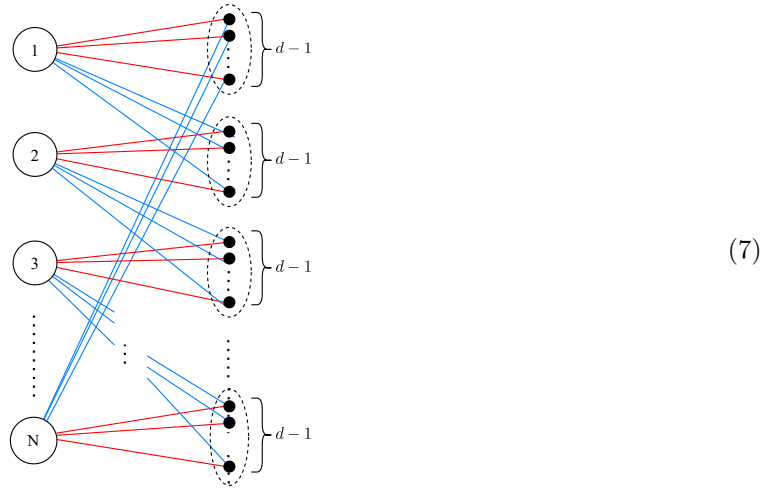
then the final state is given by the summation of the $(d-1)$ -to-one matchings between the circles and dots of the given bigraph, which correspond to the terms of the final state. This property is directly shown with the following identity

$$(\hat{a}_0)^l (\hat{a}_{\tilde{d-1}})^{d-1-l} \prod_{s=0}^{d-1} \hat{a}_s^\dagger |vac\rangle = (-1)^{d-1-l} \frac{l!(d-1-l)!}{\sqrt{d^{d-2}}} \hat{a}_{\tilde{d-1-l}}^\dagger |vac\rangle \quad (l \in \{0, 1, \dots, d-1\}) \quad (6)$$

and its corresponding graph identity.

The property is essential to find entanglement generation schemes, because our sculpting bigraphs have N circles and $(d-1)N$ dots, whose structures are set so that only $(d-1)$ -to-one matchings contribute to the final state in the d -level sculpting protocol. This is a generalization of EPM bigraphs, in which only perfect matchings contribute to the final state by the two-level sculpting protocol [25].

An example that satisfies the above restriction (5) is already given in Ref. [20],



which corresponds to the sculpting scheme to generate N -partite qudit GHZ state (note that the cyclic symmetry of GHZ state is reflected in the graph).

3 Sculpting schemes through the graph symmetries

In this section, we present sculpting bigraphs of N circles and $(N-1)N$ dots that generate $|\mathcal{S}_N\rangle$ and $|D^N(1, 1, \dots, 1)\rangle$. We will impose the total (anti-) symmetry under the circle label exchanges to those graphs, which directly corresponds to the total (anti-) symmetry under the spatial modes of the final target states. To see this intuitively, note that the total (anti-) symmetry is decided by $\frac{N(N-1)}{2}$ -pairs of relations. We can impose such relations to graphs with $N(N-1)$ edges that connect dots and circles, hence two edges attached to two dots are combined to produce such (anti-) symmetric property to graphs.

3.1 Totally anti-symmetric sculpting bigraph

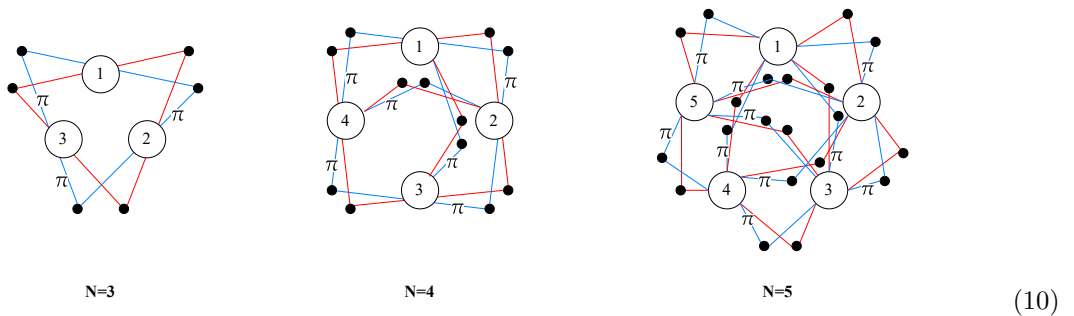
To make the sculpting bigraph totally anti-symmetric, we use the following subgraph:

$$= (\hat{a}_{j,\bar{0}}^\dagger + \hat{a}_{k,\bar{0}}^\dagger)(\hat{a}_{j,\widetilde{N-1}}^\dagger - \hat{a}_{k,\widetilde{N-1}}^\dagger) \quad (j < k). \quad (8)$$

This subgraph is anti-symmetric under the exchange of modes j and k . Since $j, k \in \{1, 2, \dots, N\}$, there are $\frac{N(N-1)}{2}$ subgraphs that construct the totally anti-symmetric sculpting bigraphs. This sculpting bigraph is equivalent to the sculpting operator

$$\hat{A}_N^{\mathcal{S}} = \prod_{j < k=0}^{N-1} (\hat{a}_{j,\bar{0}}^\dagger + \hat{a}_{k,\bar{0}}^\dagger)(\hat{a}_{j,\widetilde{N-1}}^\dagger - \hat{a}_{k,\widetilde{N-1}}^\dagger). \quad (9)$$

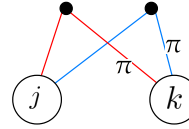
The sculpting bigraphs for $N = 3, 4$, and 5 are drawn as



It is direct to see that this bigraph is anti-symmetric under any exchange between two circles by the anti-symmetric property of the subgraph (8), which also can be directly checked in the operator side. Since the initial state $|Sym_{N,d}\rangle$ is totally symmetric, we can see that the final state is totally anti-symmetric.

3.2 N -partite N -level Dicke state $|D^N(\underbrace{1, 1, \dots, 1}_N)\rangle$ sculpting bigraph

For the generation of the totally symmetric state $|D^N(\underbrace{1, 1, \dots, 1}_N)\rangle$, we use a slightly different subgraph

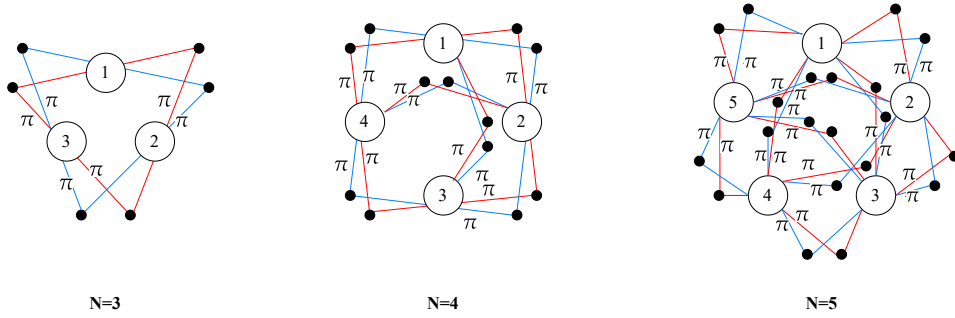


$$= (\hat{a}_{j,0}^\dagger - \hat{a}_{k,0}^\dagger)(\hat{a}_{j,N-1}^\dagger - \hat{a}_{k,N-1}^\dagger). \quad (11)$$

$\frac{N(N-1)}{2}$ of the above subgraphs constitute the Dicke sculpting bigraph, which is equivalent to the sculpting operator

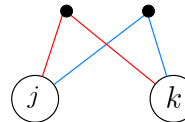
$$\hat{A}^{D_1} = \prod_{j < k=0}^{N-1} (\hat{a}_{j,0}^\dagger - \hat{a}_{k,0}^\dagger)(\hat{a}_{j,N-1}^\dagger - \hat{a}_{k,N-1}^\dagger). \quad (12)$$

The sculpting bigraphs for $N = 3, 4,$ and 5 are drawn as



To see that this type of bigraph generates $|D^N(\underbrace{1, 1, \dots, 1}_N)\rangle$, we need to divide two subgraphs that are just made of the same color of edges, which correspond to the operators $\prod_{j < k=0}^{N-1} (\hat{a}_{j,0} - \hat{a}_{k,0})$ and $\prod_{j < k=0}^{N-1} (\hat{a}_{j,N-1} - \hat{a}_{k,N-1})$. These operators are totally anti-symmetric under the exchange of spatial modes respectively, which combine to make the overall operator $A_N^{D_1}$ symmetric. This implies that in each operator terms of the same order of annihilation operators cancel with each other to conserve the anti-symmetry. Hence, when the operator is applied to the initial state, the final state consists of terms whose internal states are all different with each other, which is $|D^N(\underbrace{1, 1, \dots, 1}_N)\rangle$.

In addition, it is worth mentioning that



$$= (\hat{a}_{j,0}^\dagger + \hat{a}_{k,0}^\dagger)(\hat{a}_{j,N-1}^\dagger + \hat{a}_{k,N-1}^\dagger) \quad (13)$$

also generates another totally symmetric state. However, since $\prod_{j < k=0}^{N-1} (\hat{a}_{j,0} + \hat{a}_{k,0})$ and $\prod_{j < k=0}^{N-1} (\hat{a}_{j,N-1}^\dagger + \hat{a}_{k,N-1}^\dagger)$ are both symmetric, the final state is made of more terms. For example, for $N = 3$, the final

state is given by

$$\begin{aligned}
& \prod_{j < k = 0}^2 (\hat{a}_{j,0}^\dagger + \hat{a}_{k,0}^\dagger)(\hat{a}_{j,2}^\dagger + \hat{a}_{k,2}^\dagger) |Sym_{3,3}\rangle \\
& = |012\rangle + |120\rangle + |201\rangle + |210\rangle + |102\rangle + |021\rangle + |111\rangle \\
& = |D^3(1, 1, 1)\rangle + |111\rangle.
\end{aligned} \tag{14}$$

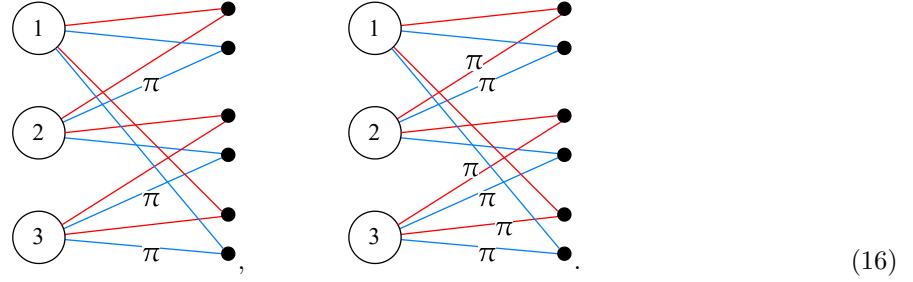
Note that this final state is similar to the qutrit tripartite Dicke state $|D_3^3\rangle$ defined in Ref. [38],

$$|D_3^3\rangle = |012\rangle + |120\rangle + |201\rangle + |210\rangle + |102\rangle + |021\rangle + 2|111\rangle. \tag{15}$$

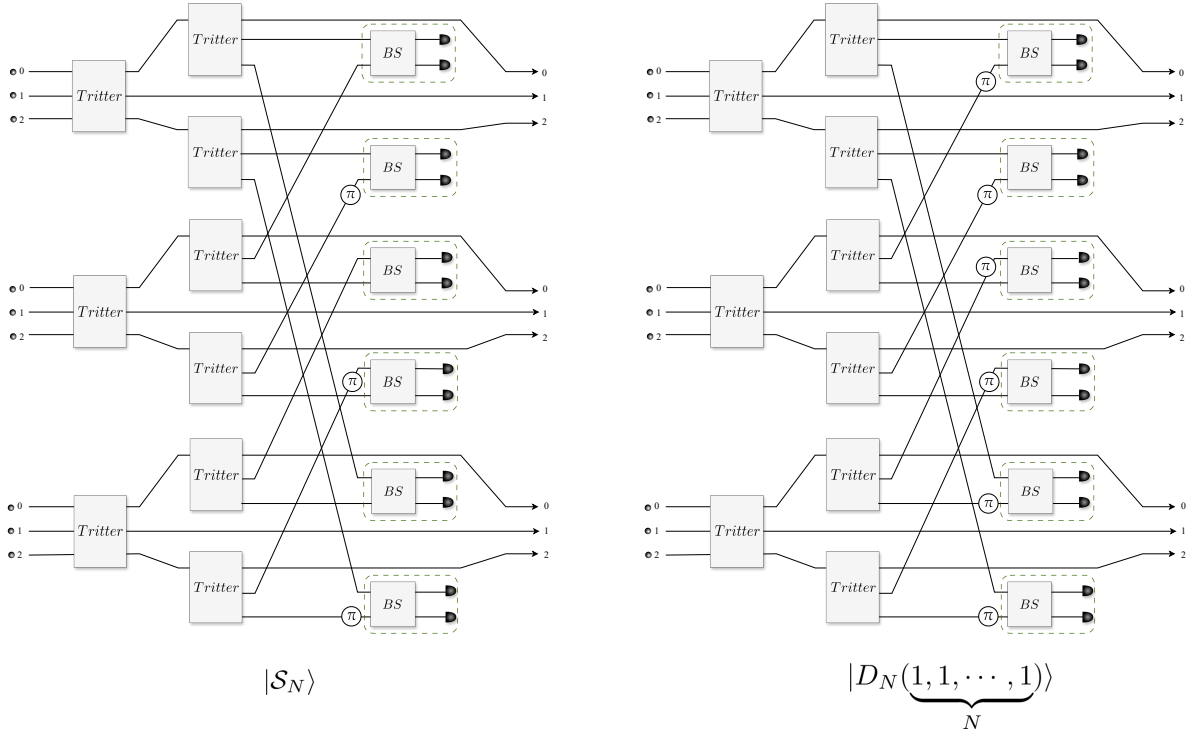
4 Linear optical schemes with heralding detectors

We design linear optical circuits with heralding detectors based on the sculpting operators introduced in Section 3. A set of translation rules from qubit sculpting bigraphs to linear optical circuits are presented in Ref. [21], which can be applied to qudit cases by straightforward generalization. Here we display the $N = 3$ examples, which is directly generalized to larger N cases.

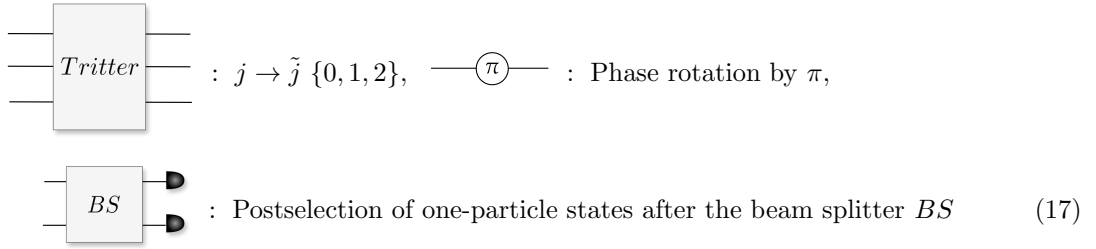
To design linear optical circuits that proceed in time from left to right, we re-array the $N = 3$ sculpting bigraphs in (10) and (13) for the $N = 3$ anti-symmetric and symmetric states as



Considering each sculpting operator as a heralding detector, the $N = d = 3$ totally anti-symmetric state is generated by the following optical circuit with triple-rail encoding:



where



Note that the operations in the dashed boxes of the above circuits play the role of subtraction operators. Wires are connected to those boxes following the structure of sculpting bigraphs (16). The success probability is $\frac{2\sqrt{6}}{3^8}$ with feed-forward at the detectors after BSs.

The N -partite N -level generalization of the above schemes is straightforward by replacing tritters with N -partite ports, whose success probability is given by $\frac{N!\sqrt{N!}}{(N^N)^N}$.

5 Discussions

In this study, we have proposed heralded schemes that generate N -partite N -level symmetric and anti-symmetric states with the LQG picture. We expect our current results serve as a foundation upon which to build interesting systematic and optimized strategies for the generation of qudit multipartite entangled states. Our graphical solutions can be considered a special group of the qudit generalization of EPM bigraphs introduced in Ref. [20], which has convenient properties that can directly correspond to the heralded generation of *qubit* multipartite entanglement. A more rigorous formalism for the *qudit* generalization of EPM bigraphs including more ancillary particles will provide abundance possibility to find more complicated qudit entangled states with less symmetries, such as absolutely maximally entangled states and qudit graph states.

Acknowledgements

This research was supported by National Research Foundation of Korea (NRF, RS-2023-00245747) and the quantum computing technology development program of the National Research Foundation of Korea (NRF) funded by the Korean government (Ministry of Science and ICT, MSIT, No.2021M3H3A103657313).

References

- [1] David P DiVincenzo. Quantum computation. *Science*, 270(5234):255–261, 1995.
- [2] Emanuel Knill, Raymond Laflamme, and Gerald J Milburn. A scheme for efficient quantum computation with linear optics. *Nature*, 409(6816):46–52, 2001.
- [3] Hans J Briegel, David E Browne, Wolfgang Dür, Robert Raussendorf, and Maarten Van den Nest. Measurement-based quantum computation. *Nature Physics*, 5(1):19–26, 2009.
- [4] Dik Bouwmeester, Jian-Wei Pan, Klaus Mattle, Manfred Eibl, Harald Weinfurter, and Anton Zeilinger. Experimental quantum teleportation. *Nature*, 390(6660):575–579, 1997.
- [5] Nicolas Gisin and Rob Thew. Quantum communication. *Nature photonics*, 1(3):165–171, 2007.
- [6] Iulia M Georgescu, Sahel Ashhab, and Franco Nori. Quantum simulation. *Reviews of Modern Physics*, 86(1):153, 2014.
- [7] Daniele Cozzolino, Beatrice Da Lio, Davide Bacco, and Leif Katsuo Oxenløwe. High-dimensional quantum communication: benefits, progress, and future challenges. *Advanced Quantum Technologies*, 2(12):1900038, 2019.

- [8] Yuchen Wang, Zixuan Hu, Barry C Sanders, and Sabre Kais. Qudits and high-dimensional quantum computing. *Frontiers in Physics*, 8:589504, 2020.
- [9] Malte C Tichy, Fernando de Melo, Marek Kuś, Florian Mintert, and Andreas Buchleitner. Entanglement of identical particles and the detection process. *Fortschritte der Physik*, 61(2-3):225–237, 2013.
- [10] Mario Krenn, Armin Hochrainer, Mayukh Lahiri, and Anton Zeilinger. Entanglement by path identity. *Physical Review Letters*, 118(8):080401, 2017.
- [11] Seungbeom Chin and Joonsuk Huh. Entanglement of identical particles and coherence in the first quantization language. *Physical Review A*, 99(5):052345, 2019.
- [12] Mariana R Barros, Seungbeom Chin, Tanumoy Pramanik, Hyang-Tag Lim, Young-Wook Cho, Joon-suk Huh, and Yong-Su Kim. Entangling bosons through particle indistinguishability and spatial overlap. *Optics Express*, 28(25):38083–38092, 2020.
- [13] Pawel Blasiak and Marcin Markiewicz. Entangling three qubits without ever touching. *Scientific Reports*, 9, 2019.
- [14] Donghwa Lee, Tanumoy Pramanik, Seongjin Hong, Young-Wook Cho, Hyang-Tag Lim, Seungbeom Chin, and Yong-Su Kim. Entangling three identical particles via spatial overlap. *Optics Express*, 30(17):30525–30535, 2022.
- [15] Stefanie Barz, Gunther Cronenberg, Anton Zeilinger, and Philip Walther. Heralded generation of entangled photon pairs. *Nature Photonics*, 4(8):553–556, 2010.
- [16] Scott B Papp, Kyung Soo Choi, Hui Deng, Pavel Lougovski, SJ Van Enk, and HJ Kimble. Characterization of multipartite entanglement for one photon shared among four optical modes. *Science*, 324(5928):764–768, 2009.
- [17] Jonas Zeuner, Aditya N Sharma, Max Tillmann, René Heilmann, Markus Gräfe, Amir Moqanaki, Alexander Szameit, and Philip Walther. Integrated-optics heralded controlled-not gate for polarization-encoded qubits. *npj Quantum Information*, 4(1):13, 2018.
- [18] Jin-Peng Li, Xuemei Gu, Jian Qin, Dian Wu, Xiang You, Hui Wang, Christian Schneider, Sven Höfling, Yong-Heng Huo, Chao-Yang Lu, et al. Heralded nondestructive quantum entangling gate with single-photon sources. *Physical Review Letters*, 126(14):140501, 2021.
- [19] Dat Thanh Le, Warit Asavanant, and Nguyen Ba An. Heralded preparation of polarization entanglement via quantum scissors. *Physical Review A*, 104(1):012612, 2021.
- [20] Seungbeom Chin, Yong-Su Kim, and Marcin Karczewski. Graph approach to entanglement generation by boson subtractions. *arXiv preprint arXiv:2211.04042*, 2022.
- [21] Seungbeom Chin, Marcin Karczewski, and Yong-Su Kim. From graphs to circuits: Optical heralded generation of N -partite GHZ and W states. *arXiv preprint arXiv:2310.10291*, 2023.
- [22] Seungbeom Chin. Boson subtraction as an alternative to fusion gates for generating graph states. *arXiv preprint arXiv:2306.15148*, 2023.
- [23] Shuai Zhao, Wen-Fei Cao, Yi-Zheng Zhen, Changchen Chen, Li Li, Nai-Le Liu, Feihu Xu, and Kai Chen. Higher amounts of loophole-free bell violation using a heralded entangled source. *New Journal of Physics*, 21(10):103008, 2019.
- [24] Morgan M Weston, Sergei Slussarenko, Helen M Chrzanowski, Sabine Wollmann, Lynden K Shalm, Varun B Verma, Michael S Allman, Sae Woo Nam, and Geoff J Pryde. Heralded quantum steering over a high-loss channel. *Science advances*, 4(1):e1701230, 2018.
- [25] Seungbeom Chin, Yong-Su Kim, and Sangmin Lee. Graph picture of linear quantum networks and entanglement. *Quantum*, 5:611, 2021.
- [26] John van de Wetering. Zx-calculus for the working quantum computer scientist. *arXiv preprint arXiv:2012.13966*, 2020.

- [27] Jacob Biamonte. Lectures on quantum tensor networks. *arXiv preprint arXiv:1912.10049*, 2019.
- [28] Marc Hein, Wolfgang Dür, Jens Eisert, Robert Raussendorf, M Nest, and H-J Briegel. Entanglement in graph states and its applications. *arXiv preprint quant-ph/0602096*, 2006.
- [29] Mario Krenn, Xuemei Gu, and Anton Zeilinger. Quantum experiments and graphs: Multiparty states as coherent superpositions of perfect matchings. *Physical Review Letters*, 119(24):240403, 2017.
- [30] Adán Cabello. N-particle N-level singlet states: some properties and applications. *Physical review letters*, 89(10):100402, 2002.
- [31] Matthias Fitzi, Nicolas Gisin, and Ueli Maurer. Quantum solution to the byzantine agreement problem. *Physical Review Letters*, 87(21):217901, 2001.
- [32] Rafael I Nepomechie and David Raveh. Qudit Dicke state preparation. *arXiv preprint arXiv:2301.04989*, 2023.
- [33] M Enríquez, I Wintrowicz, and Karol Życzkowski. Maximally entangled multipartite states: a brief survey. In *Journal of Physics: Conference Series*, volume 698, page 012003. IOP Publishing, 2016.
- [34] Zihao Li, Yun-Guang Han, Hao-Feng Sun, Jiangwei Shang, and Huangjun Zhu. Verification of phased dicke states. *Physical Review A*, 103(2):022601, 2021.
- [35] Géza Tóth and Morgan W Mitchell. Generation of macroscopic singlet states in atomic ensembles. *New Journal of Physics*, 12(5):053007, 2010.
- [36] Matteo Piccolini, Marcin Karczewski, Andreas Winter, and Rosario Lo Franco. Robust generation of N -partite N -level singlet states by identical particle interferometry. *arXiv preprint arXiv:2312.17184*, 2023.
- [37] Marcin Karczewski, Su-Yong Lee, Junghee Ryu, Zakarya Lasmar, Dagomir Kaszlikowski, and Paweł Kurzyński. Sculpting out quantum correlations with bosonic subtraction. *Physical Review A*, 100(3):033828, 2019.
- [38] Wiesław Laskowski, Junghee Ryu, and Marek Żukowski. Noise resistance of the violation of local causality for pure three-qutrit entangled states. *Journal of Physics A: Mathematical and Theoretical*, 47(42):424019, 2014.